SUPERCONDUCTIVITY, INCLUDING HIGH-TEMPERATURE SUPERCONDUCTIVITY

Charge-flux qubit coupled to a tank circuit in a strong low-frequency electromagnetic field

V. I. Shnyrkov[a)]

B. Verkin Institute for Low Temperature Physics and Engineering of the National Academy of Sciences of Ukraine, 47 Lenin Ave., Kharkov 61103, Ukraine

W. Krech and D. Born

Friedrich Schiller University, Institute of Solid State Physics, 5 Helmholtzweg, Jena D-07743, Germany

V. V. Serebrovsky

South-West State University, st. 50 let Oktyabrya, 94, Kursk 305040, Russia

O. G. Turutanov

B. Verkin Institute for Low Temperature Physics and Engineering of the National Academy of Sciences of Ukraine, 47 Lenin Ave., Kharkov 61103, Ukraine
(Submitted April 10, 2014)
Fiz. Nizk. Temp. **40**, 1331–1342 (December 2014)

A superconducting charge-flux qubit coupled to a high-Q tank circuit was studied in a low-frequency electric field. A fine structure of the multiphoton resonance lines and quantum interference effects associated with the excitation of a quasi-two-level system due to the Landau–Zener–Stückelberg tunneling was observed. The results obtained for multiphoton resonant excitations and low-frequency oscillations of the average occupation of quantum levels were compared using different parameters of the measuring circuit. The mechanism responsible for the fine structure of resonance lines was considered. The method to measure the impedance arising in the tank circuit due to the oscillations of the superconducting current in the qubit and the main sources of decoherence were discussed. © *2014 AIP Publishing LLC*. [http://dx.doi.org/10.1063/1.4904425]

1. Introduction

Designing a quantum information processor based on any physical system requires the establishment of $N \gg 1$ interacting with each other and selectively controllable quantum bits (qubits), the states of which can be measured in the course of computation. Measurement of the state of a single qubit is one of the main problems in the development of design concepts of a quantum computer.[1] The theoretical analysis of fuzzy continuous quantum measurements of superconducting qubits[2–6] coupled to a resonant circuit, which was partly stimulated by experiments,[7–9] has allowed to estimate the rate of decoherence introduced by the control and measuring circuits. However, further visibility improvement in the measurements of the interference dependences, which arise due to the conservation of phase relations, remains an important challenge. Finding a solution to this problem is directly related to increasing the sensitivity of the detectors of magnetic flux and electric charge based on charge-flux qubits[10] as well as the magnetometers based on superconducting qubit detectors (rf SQUBID).[11] From the point of view of the development of experimental techniques of quantum measurements, such detectors are of interest due to the absence of quasiparticle currents in the adiabatic regime. For example, SQUBIDs can be an alternative to SQUIDs, which are now successfully used to measure the dynamics of magnetic flux in qubits.[12]

Qubits with Josephson junctions[13,14] are superconducting elements, in which a macroscopically large number of Cooper pairs are in the same quantum current state due to the Bose-Einstein condensation. On the one hand, the state of such objects can be measured with high quantum efficiency, while on the other hand, the macroscopic dimensions of the qubits are the main cause of their rapid decoherence due to the strong coupling with the environment and the measuring device.[4–16]

Recently, for phase qubits shunted by a large capacitance and inserted into a 3D microwave resonator, due to good decoupling from the excitation and reading circuits, a time of decoherence $\tau_\varphi \approx 95$ μs has been achieved.[17,18] Such times are essentially sufficient for quantum error correction, which makes the superconductive quasi-two-state coherent quantum systems of the "transmon" type[19] one of the likely candidates for constructing quantum circuits. In a 3D-"transmon" qubit, due to additional shunt capacitance ($\sim$90 pF), the ratio of the Josephson energy E_J to the charge energy E_C reaches 49. In this limit the separation between the ground and excited levels is $f_{12} = 4.2$ GHz,[18] while the Hamiltonian of the qubit is practically independent of the electric charge. This allows to suppress one of the main mechanisms of decoherence associated with charge noise.

When designing quantum charge detectors (electrometers),[20,21] the charge term in the Hamiltonian of the qubit cannot be made arbitrarily small, since it determines the conversion slope and the sensitivity of the detector. Moreover, a significant increase in the mass (capacitance) of the quantum oscillator reduces its characteristic frequency and limits its speed. Decoherence times obtained for 2D charge-flux qubits are in the range $\tau_\varphi = 10^{-8}$–10^{-7} s and, as follows from the theoretical analysis,[5] can be determined by measuring the coupling with the measurement circuit and the control gates.

In Refs. 22 and 23, it has been proposed to use the Landau-Zener-Stückelberg (LZS) interference effect,[24–27] which arises in a low-frequency electromagnetic field upon a periodic passage through the point of convergence of the adiabatic levels. In such measurements (for review see Ref. 28) the occupation of the upper level depends on the phase accumulated by the wave function between two successful tunneling events. In a number of studies using the formalism of the Bogolyubov-Krylov asymptotic expansion,[29] a quasi-classical description of the LZS effects and Rabi oscillations in superconducting qubits coupled with a high-Q tank circuit has been obtained. In particular, Refs. 30–32 have analyzed the coherent LZS dynamics of charge-flux qubits, in which the Hamiltonian depends both on the electric field (charge) and the magnetic flux. In the developed approach, the fine structure of the system behavior, which arises due to multiphoton resonances in a low-frequency electromagnetic field, can be explained.[32] For small splitting between the levels, where the tunneling probability is close to unity, the coherent LZS effects have been experimentally demonstrated for a flux qubit.[33] Using this effect, in Refs. 34–36 the decoherence times τ_φ have been estimated for charge, phase and flux qubits. For a charge-flux qubit with $E_J/E_C \approx 4$, the experimental results agree well with the theory[31,32] for short decoherence times. As has been shown in Ref. 19, this time grows exponentially with E_J/E_C. The visibility of the interference dependences obtained for qubits with small splitting is reduced due to an increased occupation of the upper level due to temperature. Therefore, from the perspective of improving the LZS interferometry method, coherent dynamics of qubits with large separation between the levels and an increased ratio E_J/E_C is of particular interest.

In this paper we report experimental results on the LZS dynamics of thin-film 2D charge-flux qubits with the separation between the ground and excited energy levels at the degeneracy point $\Delta E_{12}/h \approx 6.4$ GHz. In particular, the present paper discusses fine structure of the resonance lines in qubit spectroscopy and the results obtained in the region of multiphoton resonances in qubits with the ratio $E_J/E_C \approx$ 8–12 ("transmon" mode) in a low-frequency electromagnetic field $\omega/2\pi = 1.4$–1.5 GHz. We also discuss the issues related to the signal path, which represent the main source of spontaneous emission and decoherence in our experiment.

2. Charge-flux qubit and experimental methods

Application of the quasi-classical theory to describe the continuous fuzzy quantum measurements[2,4] on the "qubit–tank circuit" system (see the diagram in Fig. 1) allows separating the slow dynamics of the circuit from the fast dynamics of the qubit.[4–6] In this case, first the dynamics of the autonomous qubit is considered, and then, using the effective parameters, the response of the tank circuit excited by the current of a high-frequency generator I_G with a frequency f_G, close to the resonant frequency of the circuit $f_{0T} = (L_T C_T)^{-1/2}$ is found.

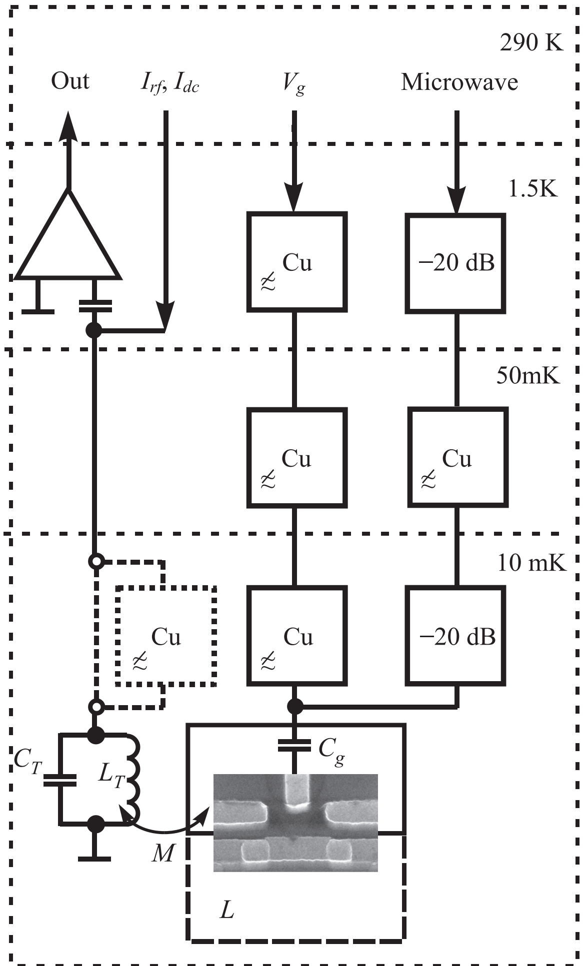

FIG. 1. Electrical diagram for continuous fuzzy quantum measurements of the characteristics of a charge-flux qubit coupled with a tank circuit L_T, C_T through a mutual inductance M. Dc and ac electric charges are induced on the island through the capacitance of the charge gate C_g by a voltage source V_g and a microwave generator. Magnetic fluxes Φ_{rf} and Φ_{dc} in the qubit inductance L are induced by the coil L_T (flux gate). The dashed line shows the filter which was inserted into the schematics to obtain an estimate of the back action of the amplifier on the qubit.

Following Refs. 5 and 6, let us write the Hamiltonian of a charge-flux qubit as

$$H = e^2(n - n_g)^2/2C_\Sigma - \varepsilon_J(\delta)\cos\varphi. \quad (1)$$

Here, the first term describes the total charge energy of the island, located between the two Josephson junctions with the capacitances C_1 and C_2 and coupled through the capacitance C_g with the charge gate. The second term is the Josephson coupling energy of the island with the superconducting circuit. Here $C_\Sigma = C_1 + C_2 + C_g$ is the total capacitance of the central part (island) of the qubit, n_g is the polarization charge (normalized by the electron charge e), $n_g e = C_g V_g$, which is induced by the voltage V_g. Dimensionless variable $n = 2N$ corresponds to the excess number of Cooper pairs N on the central electrode. The phase on the island $\varphi = (\varphi_1 - \varphi_2)/2$ is associated with the difference of the phases φ_1 and φ_2 on the individual contacts.

The Josephson coupling energy $\varepsilon_J(\delta)$ is a function of the quantum variable $\delta = \varphi_1 + \varphi_2$:

$$\varepsilon_J(\delta) = (E_{J1}^2 + E_{J2}^2 + 2E_{J1}E_{J2}\cos\delta)^{1/2}. \quad (2)$$

In the limit of a small screening current (flux) $\delta \approx \varphi_e = 2\pi\Phi_e/\Phi_0$, where φ_e is the external magnetic flux normalized by the magnetic flux quantum $\Phi_0 = h/2e$. For the concept of measurements used in the present study, an important quantity is the inverse quantum inductance of a Josephson qubit[5,6]

$$L_{nJ}^{-1}(\delta, n_g) = \left(\frac{2\pi}{\Phi_0}\right)^2 \frac{\partial^2 H}{\partial \delta^2} = \left(\frac{2\pi}{\Phi_0}\right)^2 \frac{\partial^2 E_n(\delta, n_g)}{\partial \delta^2}, \quad (3)$$

which is determined by the local curvature of the n-th energy level (surface) $E_n(\delta,n_g)$. Near the singularities ($q = e$ and $\varphi_e = \pi$), the local curvature increases and the inverse inductances in ground $L_{1J}^{-1}(\delta, n_g)$ and excited $L_{2J}^{-1}(\delta, n_g)$ states can increase significantly.[5,6] The noise induced in the qubit through the charge and flux gates and the measurement circuit average these quantities and thus reduce the effective magnitudes of the inverse inductances $L_{iJ}^{-1}(\delta, n_g) \Rightarrow \langle L_{iJ}^{-1}(\delta, n_g)\rangle_N$.[5,11]

In the measurement scheme (Fig. 1), the qubit is coupled with a high-Q ($Q \gg 1$) tank circuit $L_T C_T$ through a mutual inductance $M = k^2(L_T L)^{1/2}$, where $k \ll 1$ is the coupling coefficient. Analysis of the effect of the tank circuit shows[37] that such a coupling reduces ($\propto k^2$) splitting between the levels of the qubit, but allows registering the coherence effects even at moderate Q-factors ($Q \approx 10^3$) of the tank circuit.[32,38] When moving along the ground energy level $E_1(\delta,n_g)$ in the absence of an electromagnetic field, the variations of the quantum inverse inductance $\langle L_{iJ}^{-1}(\delta, n_g)\rangle_N$ lead to a change in the inductance of the tank circuit L_T:

$$L'_T(\delta, n_g) = L_T - M^2\langle L_{1J}^{-1}(\delta, n_g)\rangle_N. \quad (4)$$

For measurements at the resonant frequency $f_G = f'_T$ and under the condition $L\langle L_{iJ}^{-1}(\delta, n_g)\rangle_N \ll 1$, the phase shift of the voltage oscillations $\alpha_T(\delta, n_g)$ in the circuit relative to the phase of the generator current can be represented as[32,39]

$$\mathrm{tg}\,\alpha_T(\delta, n_g) \approx k^2 Q L\langle L_{iJ}^{-1}(\delta, n_g)\rangle_N. \quad (5)$$

In the present study, this approximation was used for the measurements of the qubit parameters included in the Hamiltonian (1), spectroscopy of the multiphoton resonances and recording the interference dependences.

A charge-flux qubit consists of a superconducting aluminum (Al) loop with an inductance $L \approx 0.75$ nH, closed with two Josephson tunnel Al–Al_2O_3–Al junctions. The junctions have approximately equal critical currents $I_1 \approx I_2 \approx 120$ nA and the junction capacitances $C_1 \approx C_2 \approx 2$ fF at 10 mK. Estimates of the area of the mesoscopic tunnel junctions from SEM images gave the size of 235×200 nm $\pm 10\%$. Between the contacts there is an "island" of a small volume with the characteristic temperature $T^* = \Delta_{Al}(0)/(k_B \ln N_{\mathrm{eff}}) \approx$ 125–140 mK,[40] which is coupled to the charge gate through the capacitance $C_g \approx 0.1$ fF. Here $\Delta_{Al}(0)$ is the superconducting gap in aluminum at $T \to 0$, k_B is the Boltzmann constant, and N_{eff} is the effective number of charge carriers, proportional to the volume of the island. For the samples ChQ1, ChQ2 and ChQ3, all fabricated using the same technology, the calculated values of the individual Josephson coupling energies of the tunnel junctions $E_{J1} \approx E_{J2} = I_{1,2}\Phi_0/2\pi \approx h\cdot$(55–60) GHz exceeded the calculated charging energy of a pair $E_{CP} = 4E_C = (2e)^2/2C_\Sigma \approx$ h$\cdot$(19–20) GHz and $E_{J1,2}/E_C \approx 12$, where $2e$ is the charge of a Cooper pair.

An increase in the geometric inductance L of a qubit simplifies the design of detectors, control and monitor circuits, and two-qubit quantum gates. However, with increasing L, the area of the quantization loop also increases, and so the coupling to the electromagnetic environment and, accordingly, the rate of decoherence. To reduce this effect, the superconducting quantization loops for the qubits ChQ2 and ChQ3 were fabricated as first-order gradiometers with the symmetry coefficient for the loops better than 10^4. The superconducting loop of the qubit ChQ1 was made in the form of a magnetic dipole with a size 0.5×0.5 mm (see Fig. 1). The main parameters of the measurement circuits for the three qubits are given in Table 1.

The inductance of the tank circuit L_T was fabricated as a single-layer niobium film spiral located above the qubit loop. The geometric inductance of the qubits $L \approx 0.75$ nH was chosen to be substantially smaller than the fluctuation inductance $L_F = (\Phi_0/2\pi)^2/k_B T$, which results in the dimensionless parameter $\beta_L = 2\pi L I_c/\Phi_0 \approx 0.28$, where I_c is the critical current of the junction, and uncertainty of the noise flux $\langle \Phi_N^2\rangle^{1/2} = (k_B T L)^{1/2} \approx 7.3 \times 10^{-18}$ Wb at $T \approx 10$ mK. To obtain the maximum phase response (5), the harmonic oscillations in the rf circuit were excited by a current generator at a frequency f_G, equal to the resonant frequency of the circuit $f_T = 1/2\pi(L'_T C_T)^{1/2}$ taking into account its shift due to the coupling to the qubit ($L'_T = L_T - M^2/L$).

The charge-flux qubit with a tank circuit was placed inside a superconducting cylindrical screen, which also served as a resonator, which was excited by an external microwave generator to induce an ac voltage $V(t) = V_0 \sin(\omega t + \theta)$ on the charge gate. It should be noted that when the charge gate circuit was mechanically removed, the effects associated with the microwave field, were not observed. This confirms that the microwave field acts directly on the charge gate of the qubit.

The measurement cell with a qubit was installed on the dilution refrigerator stage with a nominal temperature of 10 mK. A dc voltage V_g was applied to the charge gate of the qubit from a 10 Ω resistor, which was cooled down to $T \approx$ 100 mK, through powder filters located at the temperature levels of 50 and 10 mK. The transfer coefficient of the charge gate $(C_g/C)^2 \approx 1.8 \times 10^{-3}$ was selected such to reduce the influence of thermal fluctuations[5,41] on the decoherence rate. To reduce the spectral density of the magnetic flux noise at the current gate, the normalized transfer coefficient $(MI/\Phi_0)^2$ was reduced to 3.6×10^{-4}. The magnitudes of M and C_g were determined from the periodic dependences $\alpha_T(\Phi_e)$ and $\alpha_T(V_g)$ (see Fig. 2).

In the measurement scheme employed, the effective noise temperature of the qubit T_{eff}, found from the

TABLE 1. Main parameters of the measuring schemes for three qubits.

Sample	L (nH)	L_T (μH)	f_0 (MHz)	Q	k^2Q	M (nH)	$\lvert E_{J1} - E_{J2}\rvert/h$ (GHz)	C_g (fF)
ChQ1	0.75	0.168	27.387	700	0.44	0.437	7.5	0.097
ChQ2	0.75	0.17	28.91	516	0.56	0.37	7.28	0.092
ChQ3	0.75	0.17	29.795	350	0.385	0.44	7.28	0.092

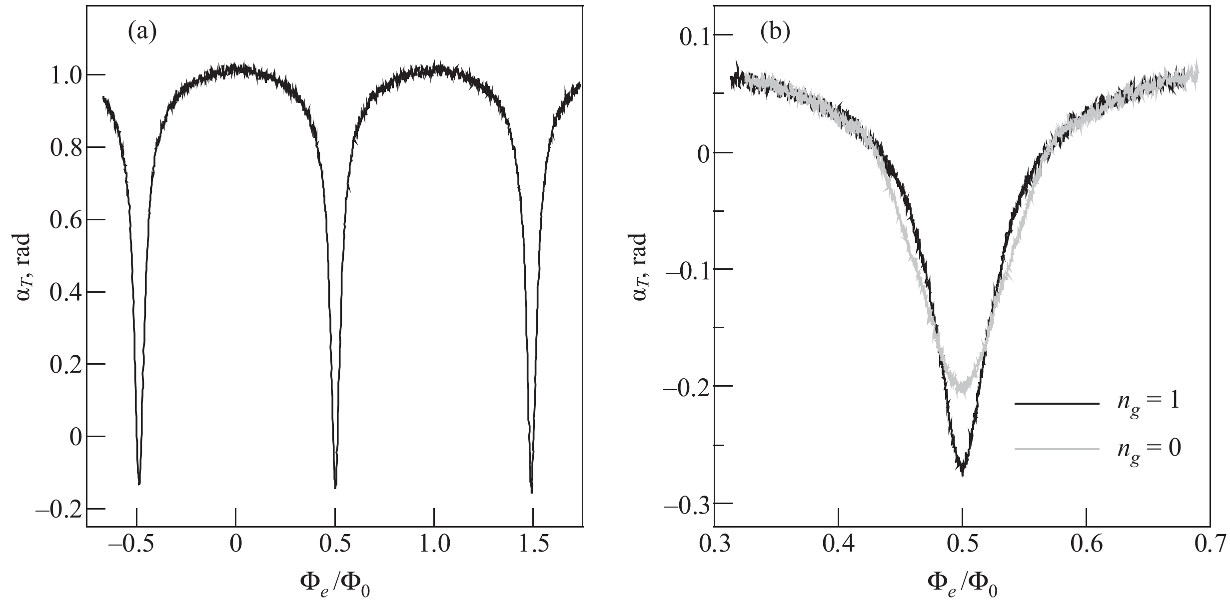

FIG. 2. Calibration of the flux and charge gates for the qubit ChQ1, carried out at the resonant frequency $f_G = f_T$ and a bath temperature $T = 10$ mK ($T_{\rm eff} \approx 75$ mK). (a) Dependence $\alpha_T(\Phi_e, n_g = 1)$, which is proportional to the derivative of the current-phase relation with a period of the current $\Delta i_{\Phi_0} = \Phi_0/M = 4.737$ μA. (b) Dependences $\alpha_T(\Phi_e)$, obtained for two values of $n_g = 0$ and 1, corresponding to the voltage difference at the charge gate $V_{g1} - V_{g2} = 3.3$ mV.

temperature dependence of the Rabi oscillation amplitude,[38] was $T_{\rm eff} = (75 \pm 15)$ mK. The decoherence time $T_2 \approx 2/\Delta\Omega_R$ obtained for the qubits ChQ2 and ChQ3 from the Rabi oscillation bandwidth $\Delta\Omega_R$ in a resonant electromagnetic field $\hbar\omega \approx |E_{J1} - E_{J2}|$ was $T_2 \approx 0.1$–0.3 μs.[38] In these measurements, the variation of the Q-factor of the tank circuit was measured by noise spectroscopy, i.e., with no current from the generator ($I_G = 0$).

Fig. 2 shows an example of calibration dependences of the voltage oscillations phase in the tank circuit coupled with the qubit ChQ1 (see Table 1) on the external magnetic flux plotted for several values of induced charge: $\alpha_T(\Phi_e, n_g = 1)$, $\alpha_T(\Phi_e, n_g = 1;0)$. To improve the signal-to-noise ratio the measurements were carried out at the amplitude of the rf generator current $I_G \approx 5 \times 10^{-3}$ $\Phi_0/(QM)$.

The values of M and C_g, obtained from such measurement for the three samples are shown in Table 1. Analysis of the dependence $\alpha_T(\varphi_e, n_g = 1)$ for the qubit ChQ1 (Fig. 2(a)) gives the Josephson energy of the junctions 25% lower than that found from the calibration measurements on the reference sample. This may be due to either the effect of noise or the magnitude of the rf magnetic flux induced in the qubit by the tank circuit. To reduce the effect of averaging the dependences (see below), in the subsequent studies the RF generator current was selected to satisfy the condition $I_G \leq 10^{-3}/\Phi_0(QM)$.

3. Qubit in a strong low-frequency electromagnetic field

For the above measurement scheme (Fig. 1), the response of a qubit (Eq. (1)) to an external low-frequency monochromatic electric field $V(t) = V_0\sin(\omega t + \theta)$ has been considered in a number of studies.[6,8,10,31,32,38] In particular, in Ref. 38 it has been shown that by rearranging the Hamiltonian by an external magnetic flux Φ_e, at an optimal amplitude V_0 at the gate of the qubit, the Rabi oscillations can be observed in the vicinity of one-, two- and three-photon resonances. On the other hand, if the frequency of the electric field is ramped, then in a dc magnetic field, due to a strong nonlinearity, multiphoton resonances with the number of photons $\gamma = 2, 3, 4, \ldots$ should be observed on the dependences $\alpha_T(\omega, \varphi_e = \pi, n_g = 1)$:

$$\gamma\hbar\omega \approx E_{J1} - E_{J2} = \Delta E_{12}. \qquad (6)$$

Variations of the phase $\alpha_T(\delta = \pi, n_g = 1, \omega)$ in a resonant field are defined by quantum-statistical averaging over the qubit states of the inverse inductance $\langle L_J^{-1}(\delta, n_g)\rangle_q$, which takes into account both the different curvature of the ground $L_{1J}^{-1}(\delta, n_g)$ and excited $L_{2J}^{-1}(\delta, n_g)$ levels and their occupation probabilities.[10,39] The physical processes and the behavior of the dependences $\alpha_T(\delta = \pi, n_g = 1, \omega)$ in the vicinity of the resonances $\gamma\hbar\omega \approx \Delta E_{12}$ for charge-flux qubits are rather similar to those found for flux qubits.[4,37,42] For low amplitudes of an electromagnetic field, the time-averaged occupation of the upper level (without considering the tank circuit) should have a Lorentzian shape with the maximum value of 1/2 at the resonance.[43] This result is consistent with our measurements in the limit of small amplitude of an ac electric field. In Ref. 9 it has been shown that for the Josephson qubits, with increasing the power of the electromagnetic field, the shape of the resonance curve changes rapidly and becomes a Gaussian dependence. In addition, an increase in the number of photons leads to a noticeable Stark shift of the resonance frequencies.[9,43]

Spectroscopic measurements for the qubit ChQ1 in the frequency range 1.3–5.6 GHz for $n_g \approx 1$ and $\Phi_e \approx \Phi_0/2$ showed the presence of such resonances, however some additional features appear in this measurements scheme. For the dependence with a relative level of the microwave radiation of -85 dBm, the resonant excitation was observed only for the two-photon resonance $2\omega \approx \omega_{12} = \Delta E_{12}/\hbar$, located near 3.0 GHz (Fig. 3). On the dependence $\alpha_T(\delta = \pi, n_g = 1, \omega)$, additional maxima and minima associated with the presence of the tank circuit in the measurement scheme were observed in the vicinity of the resonance. With the

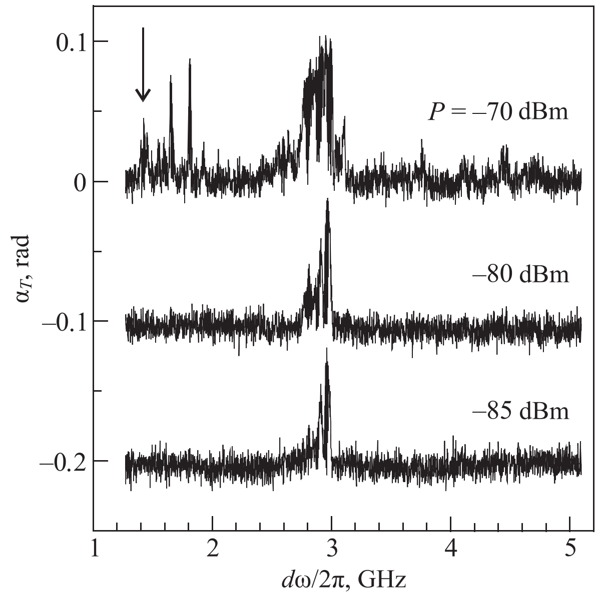

FIG. 3. Qubit ChQ1. Spectroscopy of multiphoton resonances exhibiting lines with fine structure. The spectra were obtained at $\varphi_e = \pi$, $n_g = 1$ for three different powers in the microwave path (amplitude V_0). The arrow marks a four-photon resonance observed in the vicinity of $\omega/2\pi = 1.45$ GHz upon an increase in power up to -70 dBm.

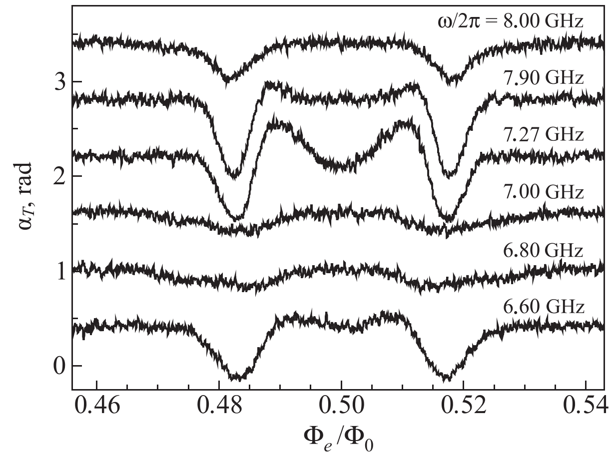

FIG. 4. Set of the dependences of the phase of rf oscillations in the tank circuit on the external magnetic flux $\alpha_T(\varphi_e)$ at a constant power of the microwave field, equal to -65 dBm. The frequency of electric field, which is varied within the set, was selected near the main resonance $\hbar\omega = \Delta E_{12}$ for the qubit ChQ2. The maximum response was obtained for the frequency $\omega/2\pi = 7.27$ GHz.

increasing power of the electromagnetic field by 5 dBm (Fig. 3, curve -80 dBm), the amplitude of the additional extrema increases. The appearance of the fine structure of resonance lines indicates the presence of the parametric conversion of energy between the qubit and the tank circuit.[4,6,10,32,38] Full quantum-mechanical model of a similar behavior of Josephson qubits has been developed in Ref. 42. Further increase in the amplitude of an electric field V_0 (Fig. 3, curve -70 dBm) results in the appearance of a resonant excitation in the vicinity of $\omega/2\pi \approx 1.4$ GHz when the energy of four absorbed photons becomes approximately equal to the separation between the quasi energy levels of the qubit. The resonance curve near 1.4 GHz also exhibits a fine structure associated with marked additional extrema, which we will consider below. As can be seen in the same dependence, in the region of two-photon resonance for such amplitude of the electric field, the saturation and broadening of the lines occurs as has been noted in Ref. 9. In the range $\omega/2\pi = 1.7$–1.9 GHz there are observed two additional narrow peaks, which are associated with geometric resonances in the measurement circuit and are almost independent of variations of the magnetic flux and charge in the qubit.

If the dipole topology of the qubit is replaced by a 2D-gradiometer so that the distance between the centers of loops d is small, than for wavelengths $\lambda \gg d$ the coupling with the electromagnetic environment becomes strongly ($\sim\sin(\pi d/\lambda)$) suppressed. To reduce the coupling with the electromagnetic environment, the consecutive studies were carried out on the samples ChQ2 and ChQ3, the quantization loops of which are designed as gradiometers, schematically denoted in Fig. 1 by the dotted line.

The frequency of the fundamental resonance for the qubit ChQ2 $\omega \approx \omega_{12} = \Delta E_{12}/\hbar$ was determined by the maximum phase response $\alpha_T(\varphi_e, n_g = 1)$ to the external magnetic flux φ_e for several frequencies of a weak microwave fields in the vicinity of the main resonance (Fig. 4). For the fundamental resonance $\gamma = 1$, the frequency dependence is quite strongly smoothed. Maximum response was found at a frequency $\omega/2\pi = 7.27$ GHz with a small offset $\Phi_e = \Phi_0(0.5 \pm 0.0125)$ from the degeneracy point.

Calculation of the value $\omega_{12}/2\pi = \Delta E_{12}/h$ for the degeneracy point $\Phi_e = \Phi_0/2$ results in $\omega_{12}/2\pi \approx 6.4$ GHz. A similar procedure, carried out near the two-photon resonance $2\omega \approx \omega_{12} = \Delta E_{12}/\hbar$, gives a value of 3.092 GHz. In this sample, a large ratio of the Josephson energy to the charge energy $E_{J1,2}/E_C \approx 12$ reduces the amplitude of charge effects. From the dependences obtained in electric fields with frequencies of 7.27 and 3.092 GHz (Fig. 5), it follows that a variation of the induced charge ($n_g = 0$; 1) results in a small phase modulation $\alpha_T(\varphi_e)$, that indicates the presence of excess noise in the system. Below we will show that the main source of noise in this scheme is the measurement circuit.

A low-frequency resonance, convenient for the observation of the LZS effect in this sample was found at a frequency of 1.473 GHz. Interference between the individual tunneling events[22,23,30–36] leads to the fact that the average occupation probability of an excited level has a double quasi-periodic dependence on the amplitude of the electric field and magnetic flux. The LZS effect arising upon the periodic passage of the degeneracy point is the electrical analog of a semi-transparent plate of an optical interferometer that separates the incident beam into two beams. For low amplitude of the electric field $V_0\sin(\omega t + \theta)$ (microwave power), the LZS tunneling probability is small, which corresponds to a plate with a low coefficient of reflection, and the interference does not occur. As the amplitude increases, so does the occupation probability of the excited level, leading to interference.

A set of the interference LZS dependences for the phase $\alpha_T(\Phi_e, V_0)$ and the amplitude $V_T(\Phi_e, V_0)$, which were obtained for the sample ChQ2 at $n_g \cong 1$ and several values of the power of the microwave generator at a frequency of 1.473 GHz, are shown in Fig. 6. The amplitude of the rf current was selected such that the signal-to-noise ratio in the tank circuit was approximately equal to one. Note that for a qubit in an ac electric field (Fig. 6, curve -57 dBm) for

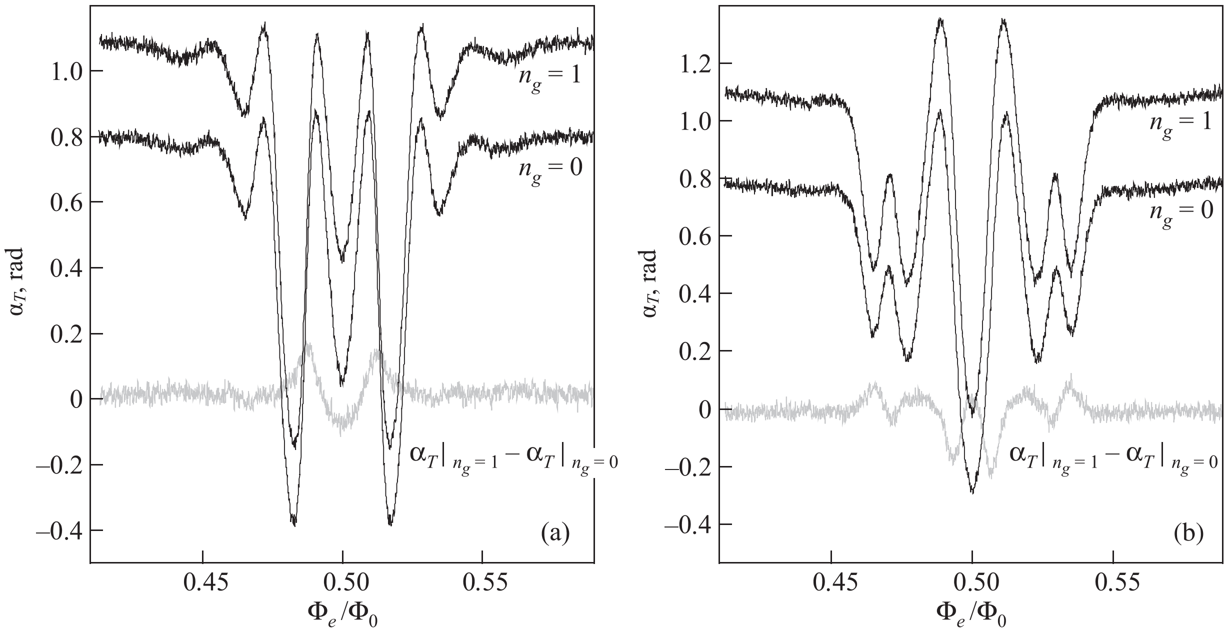

FIG. 5. Dependences $\alpha_T(\varphi_e)$ for the qubit ChQ2 obtained for the values of the electric charges $n_g = 0$ and 1 by applying an electric field with the frequencies $\omega/2\pi = 7.27$ GHz (single-photon resonance) (a) and 3.092 GHz (two-photon resonance) (b) to the charge gate. The difference of the phase signal dependences $\alpha_T(\Phi_e, n_g = 0) - \alpha_T(\Phi_e, n_g = 1)$ is shown in gray.

certain values of Φ_e near the degeneracy point, the amplitude of the voltage $V_T(\Phi_e, V_0)$ exceeds the voltage $V_T(\Phi_e)$ on the circuit at the resonance $f_G = f_0$. This effect can be explained by the energy transfer from the multiphoton Rabi oscillations with a frequency $\Omega_R(V_0) \approx f_0$ to the tank circuit. With increasing the generator power (−50, −46, −43 dBm) and, accordingly, the amplitude of the electric field on the charge gate $V_0 \sin(\omega t + \theta)$, the magnitude of the effect decreases rapidly due to a mismatch arising between these frequencies. The effective Q-factor of the peaks associated with the Rabi oscillations depends on both the choice of the operating point and the amplitude of high-frequency oscillations in the circuit. The narrowest peaks obtained by noise spectroscopy ($I_G = 0$) at the charge degeneracy point lead to the estimate of decoherence time $\tau_\varphi = 0.3$ μs. A similar interference qubit response to a weak electric field $V_0\sin(\omega t + \theta)$ was also observed in the sample ChQ3.

For the analysis of the fine structure of multiphoton resonance lines (see Fig. 3), the measurements of $\alpha_T(\Phi_e, V_0)$ and $V_T(\Phi_e, V_0)$ were carried out at discrete frequencies of the microwave generator $\omega/2\pi$, located in the vicinity of the multiphoton resonance. In these measurements, the amplitude of the rf current was increased three-fold as compared with the measurements on ChQ2 (Fig. 6) and was practically equal to the current used in the spectroscopic experiments on multiphoton resonances (Fig. 3). On the one hand, increasing the rf power improves the signal-to-noise ratio. On the other hand it leads to a characteristic smoothing of the peaks due to averaging of the local curvature over the amplitude of the rf current. A set of curves $\alpha_T(\Phi_e, V_0)$, obtained with a frequency increment $\Delta\omega/2\pi \cong 5$ MHz at a constant power of the microwave generator, is shown in Fig. 7(b). It can be seen from these curves that at $\Phi_e \approx \Phi_0/2$, the phase on the tank circuit takes the maximum (1.460 GHz—«peak») and minimum (1.465 GHz—«dip») values upon small changes in frequency. This effect is associated with a decrease in the population of the upper energy level upon a slight increase in the detuning from the multiphoton resonance frequency. This explains the appearance of fine structure in the spectroscopic measurements conducted by sweeping the frequency of an electric field.

Fig. 7(a) shows a set of amplitude dependences $V_T(\Phi_e, V_0)$, measured for the same frequencies of an ac electric field. It can be seen that for all the curves the amplitude of voltage oscillations in the tank circuit $V_T(\Phi_e)$ can considerably exceed the resonance value. Since the frequency of the rf generator was selected from the condition $f_G = f_0$, an increase in the amplitude of the oscillations requires an additional energy source with a frequency close to f_0. Such a source is the multiphoton Rabi oscillations, the frequency of which, $\Omega_R(V_0)$ depends on both the amplitude of the electric field $V_0\sin(\omega t + \theta)$ on the charge gate and the detuning of the frequency ω from the multiphoton resonance. Low-frequency dynamic processes in the region of multiphoton resonances have been considered in several studies.[4,6,31,38,44–46] The conversion of the energy of a microwave field into low-frequency occupation oscillations leads, depending on the phase, to the observed effect of increasing or decreasing the amplitude of the oscillations in the tank circuit,[4,6] recently dubbed "Sisyphus attenuation and amplification".[42,45]

The visibility of the interference dependences is determined both by the natural decoherence time of the qubit and the decoherence introduced by the measurement system.[5,41] Magnetic flux and electric charge noise induced in the qubit through the control gates can be significantly suppressed by reducing the corresponding coupling coefficients. However, the coupling coefficient between the qubit and the measuring circuit during continuous fuzzy measurements cannot be arbitrarily small and should be selected from the condition $k^2Q \approx 1$. In this case, the uncertainty of the noise flux in the qubit due to the tank circuit with a temperature T_T and the radiation temperature of the first stage of the amplifier, built using high electron mobility transistors (HEMT), can be written as

$$\Phi_{TN} \approx [k_B(T_T + T_A^{\rm irr})LQ^{-1}]^{1/2}, \quad k^2Q = 1. \qquad (7)$$

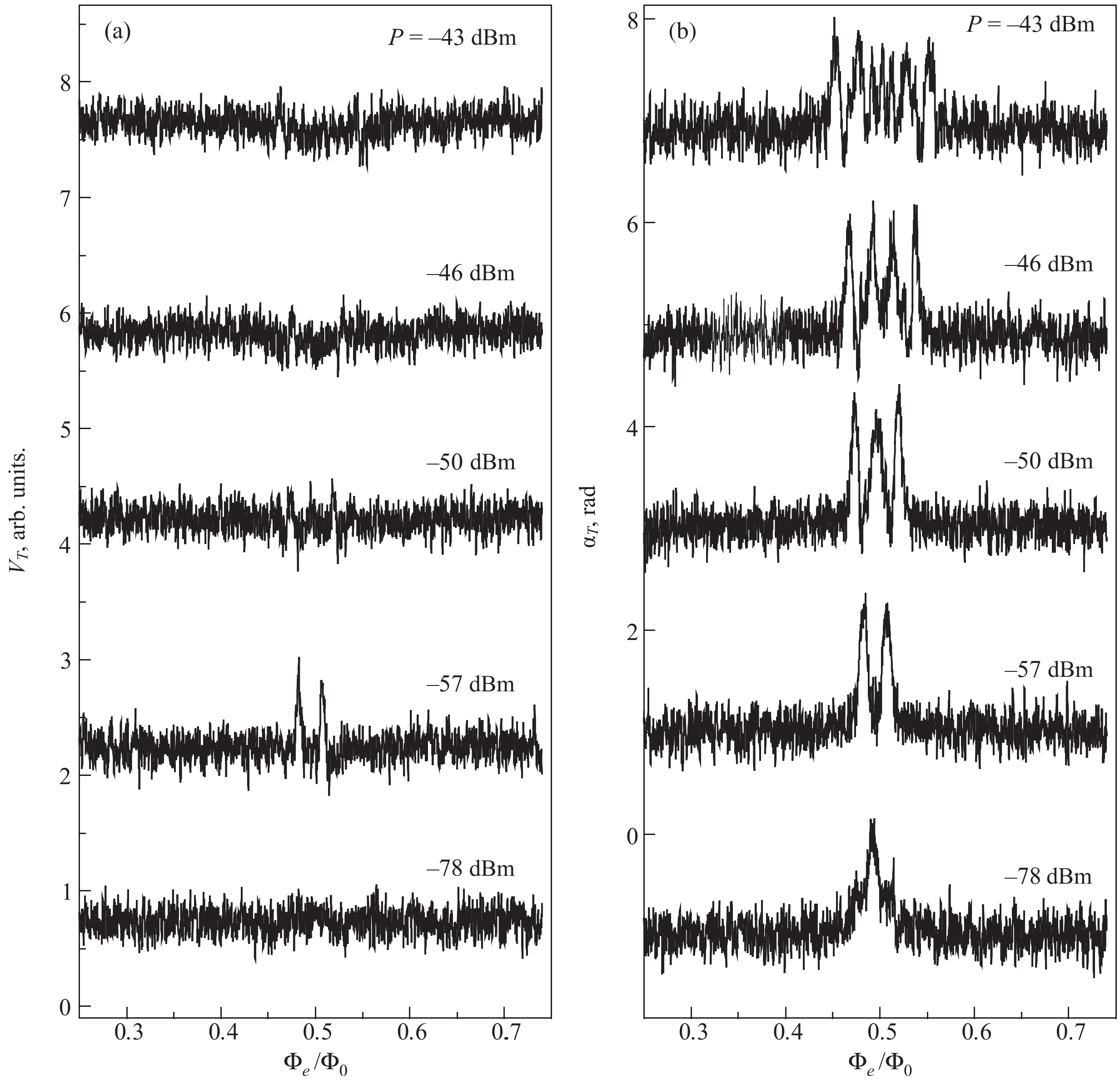

FIG. 6. Double quasi-periodic interference LZS dependence obtained for the sample ChQ2 in an electric field with a frequency $\omega/2\pi = 1.473$ GHz under the condition $f_G = f_0$. The dependences of the rf voltage in the circuit on the external magnetic flux: the amplitude $V_T(\Phi_e, V_0)$ (a) and $\alpha_T(\Phi_e, V_0)$ (b). The power of the microwave field, which generates an ac voltage on the charge gate, varies between the curves in the set. Narrow peaks ($3.6 \times 10^{-3}\Phi_0$) associated with the multiphoton Rabi oscillations are visible on the dependence $V_T(\Phi_e, V_0)$ at -57 dBm

In this expression, the ultra-wideband thermal radiation of the transistor is described by an effective temperature T_A^{irr}, which depends on the power dissipation of the dc current P_{dc} and the coefficient of capacitive input coupling S_{12}, which is proportional to the drain-gate capacitance $C \approx 0.02$ pF. An estimate of $T_A^{\text{irr}}(P_{dc})$ from the characteristic width of the interference peaks gives $T_A^{\text{irr}} \approx 3$ K.

To check the back-action of the measuring circuit on the qubit, a broadband filter based on oxidized copper powder (average particle size of 10 μm) with attenuation of 20 dB at 18 GHz, cooled down to 10 mK, was installed between the cooled amplifier and the tank circuit. The filter efficiency is demonstrated in Fig. 8, which shows the dependence of the superconducting current phase for the charge-phase qubit measured before and after installing the filter. In this scheme, the 3 cm long powder filter serves the same function as the two circulators, placed between the sample and the amplifier in Refs. 17 and 18, and results in a threefold reduction in the influence of the measuring circuit.

The obtained results indicate that in the above scheme of continuous fuzzy quantum measurements of charge-phase qubits in the "transmon" regime, the dynamic characteristics, decoherence times, and the visibility of the interference peaks studied in the region of multiphoton resonances are largely determined by the excessive temperatures T_A^{irr} and T_T of the measuring circuit.

4. Discussion

We observed fine structure of multiphoton resonance lines in spectroscopy and double interferograms associated with the excitation of quasi-two-level systems due to Landau-Zener-Stückelberg tunneling. In the vicinity of the multiphoton resonances for certain values of the amplitude of a low frequency electric field V_0, multi-photon Rabi oscillations in the qubits ChQ2 and ChQ3 appeared. In this region, $\Omega_R(V_0) \approx f_T$, an increase (decrease) in the voltage $V_T(\Phi_e)$ was observed due to parametric energy transfer between the qubit and the tank circuit.

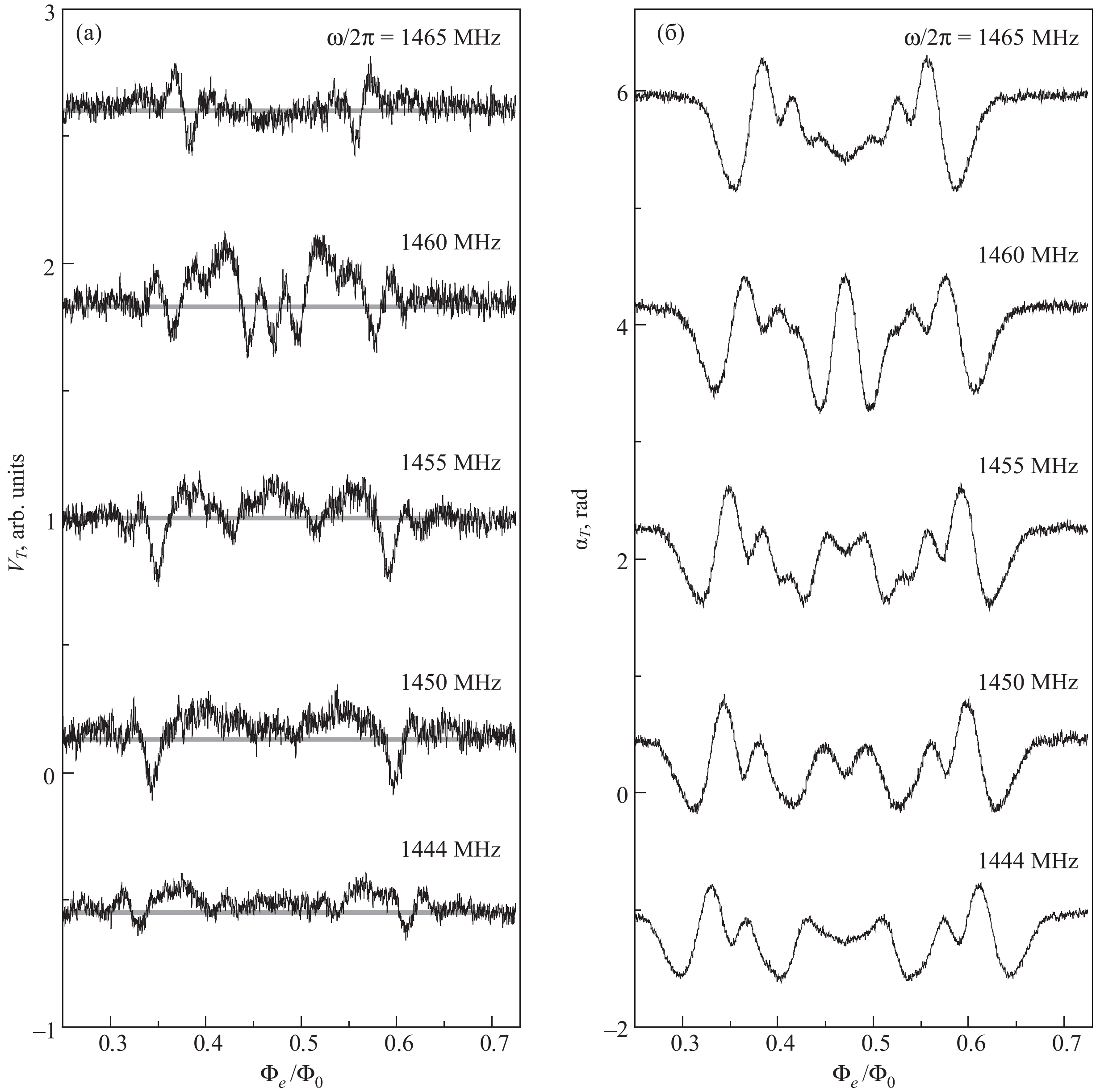

FIG. 7. Set of the interference LZS dependences of the amplitude $V_T(\Phi_e, V_0 = \text{const})$ (a) and the phase $\alpha_T(\Phi_e, V_0 = \text{const})$ (b) on the external magnetic flux for the sample ChQ3. The set was obtained for different values of the frequency of an electric field $V_0\sin(\omega t + \theta)$. The power of the microwave generator was −63 dBm for all curves. The multiphoton resonance frequency was 1.444 GHz. Gray line indicates the maximum voltage on the tank circuit at the resonance condition $f_G = f_0$ in the absence of an ac electric field.

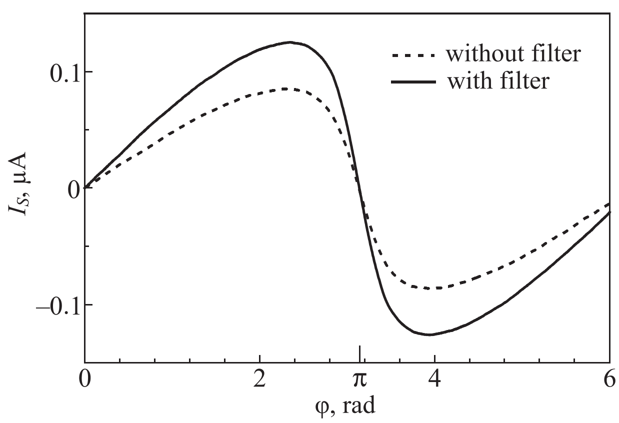

FIG. 8. Back-action effect of the measuring circuit on the qubit. Current-phase relation for the charge-flux qubit were obtained in the measurement circuit schematically shown in Fig. 1, before and after a 3 cm powder filter was installed in the measuring circuit.

As follows from the LZS interference dependences shown in Fig. 7(b), the phase signal $\alpha_T(\Phi_e, V_0 = \text{const})$ can have either "maximum" or "minimum" at $\Phi_e = \Phi_0/2$ depending on the frequency of the electric field near the multiphoton resonance. This behavior completely explains the appearance of fine structure upon sweeping the frequency of an electric field in the spectroscopic studies.

The maximum decoherence time for the sample ChQ2 with $E_{J1,2}/E_C \approx 12$, obtained from the Q-factor modulation by the Rabi oscillations (at $I_G = 0$) did not exceed $\tau_\varphi \approx 3 \times 10^{-7}$ s. The analysis of the back action of the measuring circuit on the qubit showed that the main source of decoherence time reduction and broadening of the interference peaks is the cooled HEMT-amplifier.

Using a 3 cm long coaxial powder filter in the scheme (Fig. 1), which was directly connected into the measuring circuit, increased the magnitude of the derivative of the current–phase dependence at $\varphi_e = \pi$ by 1.7-fold (Fig. 8). The dc power consumed by the amplifier results in the heating of the transistor, which necessitate placing of the amplifier stage at $T \approx 1.5$ K at a distance of 30 cm from the qubit (Fig. 1). In this case, the noise temperature of the circuit, a part of which is located at $T \leq 1.5$ K, is 300–400 mK. An estimate of the effective temperature of the transistor chips obtained from Eq. (7) gives $T_A^{\rm irr} \approx 3$K and the effective noise temperature of the qubit of 75 mK.

A substantial narrowing of the width of the interference peaks (a visibility increase) can be expected when using cooled HEMT-amplifiers with a power $P_{dc} \approx 1$ μW[47] at operating frequencies up to 500 MHz. This is due to two factors. Firstly, in this operational mode of the transistor, the temperature of the electron gas decreases significantly. Secondly, an amplifier with a power $P_{dc} \approx 1$ μW may be positioned in a dilution refrigerator in the temperature range $T \leq 100$ mK, which would allow to reduce the temperature of the tank circuit down to $T_T \leq 30$ mK. Furthermore, the decrease of the effective temperature of the qubit reduces the decoherence rate associated with the charge noise of the $1/f$ type, which is proportional to T^2.[48]

The above results and the analysis show that filtering, reduction of the coupling coefficient between the qubit and the tank circuit (by increasing f_0 up to $\sim$0.5 GHz and $Q \sim (3–5) \times 10^3$), and the use of HEMT-amplifiers with a microwatt input power allow to reduce the effective noise temperature to 20–25 mK within the technique of continuous fuzzy measurements of a qubit (or a system of coupled qubits).[49,50]

The authors are grateful to E. Ilyichev, A. A. Soroka, S. N. Shevchenko, and A. N Omelyanchuk for fruitful discussions.

This work was partially supported by the grants of the NAS of Ukraine (Project No. NANO-4/14) and the Deutsche Forschungsgemeinschaft (Contract No. KR 1172/9-2).

[a]Email: shnyrkov@ilt.kharkov.ua

[1]K. A. Valiev and A. A. Kokin, "Quantum computers: Hopes and reality," *Regular and Chaotic Dynamics* (Scientific Publishing Center, Izhevsk, 2001) (in Russian).
[2]A. N. Korotkov and D. V. Averin, Phys. Rev. B **64**, 165310 (2001).
[3]A. M. van den Brink, Europhys. Lett. **58**, 562 (2002).
[4]A. Yu. Smirnov, Phys. Rev. B **68**, 134514 (2003).
[5]A. B. Zorin, Zh. Eksp. Teor. Fiz. **125**, 1423 (2004) [JETP **98**, 1250 (2004)].
[6]W. Krech, D. Born, V. I. Shnyrkov, Th. Wagner, M. Grajcar, E. Il'ichev, H.-G. Meyer, and Y. Greenberg, IEEE Trans. Appl. Supercond. **15**, 876 (2005).
[7]E. Il'ichev, N. Oukhanski, A. Izmalkov, Th. Wagner, M. Grajcar, H.-G. Meyer, A. Yu. Smirnov, A. M. van den Brink, M. H. S. Amin, and A. M. Zagoskin, Phys. Rev. Lett. **91**, 097906 (2003).
[8]D. Born, V. I. Shnyrkov, W. Krech, Th. Wagner, E. Il'ichev, M. Grajcar, U. Hübner, and H.-G. Meyer, Phys. Rev. B **70**, 180501 (2004).
[9]D. I. Schuster, A. Wallraff, A. Blais, L. Frunzio, R.-S. Huang, J. Majer, S. M. Girvin, and R. J. Schoelkopf, Phys. Rev. Lett. **94**, 123602 (2005).
[10]V. I. Shnyrkov, A. A. Soroka, and W. Krech, Fiz. Nizk. Temp. **35**, 829 (2009) [Low Temp. Phys **35**, 652 (2009)].
[11]V. I. Shnyrkov, A. A. Soroka, and O. G. Turutanov, Phys. Rev. B **85**, 224512 (2012).
[12]A. Lupascu, S. Saito, T. Picot, P. C. De Groot, C. J. M. Harmans, and J. E. Mooij, Nat. Phys. **3**, 119 (2007).
[13]Yu. Makhlin, G. Schön, and A. Shnirman, Fortschr. Phys. **48**, 1043 (2000).
[14]J. Clarke and F. K. Wilhelm, Nature **453**, 1031 (2008).
[15]L. Tian, S. Lloyd, and T. P. Orlando, Phys. Rev. B **65**, 144516 (2002).
[16]C. M. Wilson, T. Duty, F. Persson, M. Sandberg, G. Johansson, and P. Delsing, Phys. Rev. Lett. **98**, 257003 (2007).
[17]H. Paik, D. I. Schuster, L. S. Bishop, G. Kirchmair, G. Catelani, A. P. Sears, B. R. Johnson, M. J. Reagor, L. Frunzio, L. I. Glazman, S. M. Girvin, M. H. Devoret, and R. J. Schoelkopf, Phys. Rev. Lett. **107**, 240501 (2011).
[18]C. Rigetti, J. Gambetta, S. Poletto, B. L. T. Plourde, J. M. Chow, A. D. Córcoles, J. A. Smolin, S. T. Merkel, J. R. Rozen, G. A. Keefe, M. B. Rothwell, M. B. Ketchen, and M. Steffen, Phys. Rev. B **86**, 100506(R) (2012).
[19]J. Koch, T. M. You, J. Gambetta, A. A. Houck, D. I. Schuster, J. Majer, A. Blais, M. H. Devoret, S. M. Girvin, and R. J. Schoelkopf, Phys. Rev. A **76**, 042319 (2007).
[20]W. Krech, M. Grajcar, D. Born, and I. Zhylyaev, Phys. Lett. A **303**, 352 (2002).
[21]A. B. Zorin, Physica C **368**, 284 (2002).
[22]A. V. Shytov, D. A. Ivanov, and M. V. Feigel'man, Eur. Phys. J. B **36**, 263 (2003).
[23]J. Q. You and F. Nori, Phys. Rev. B **68**, 064509 (2003).
[24]L. D. Landau, Phys. Z. Sowjetunion **1**, 88 (1932).
[25]C. Zener, Proc. R. Soc. London, Ser. A **137**, 696 (1932).
[26]E. C. G. Stückelberg, Helv. Phys. Acta **5**, 369 (1932).
[27]F. Di Giacomo and E. E. Nikitin, Usp. Fiz. Nauk **175**, 545 (2005) [Phys.-Usp **48**, 515 (2005)].
[28]S. N. Shevchenko, S. Ashhab, and F. Nori, Phys. Rev. B **85**, 094502 (2012).
[29]N. N. Bogoliubov and Yu. A. Mitropolsky, *Asymptotic Methods in the Theory of Non-Linear Oscillations* (Nauka, Moscow, 1974), English Translation of 1st ed., Gordon & Breach, New York (1961).
[30]S. N. Shevchenko, A. S. Kiyko, A. N. Omelyanchouk, and W. Krech, Fiz. Nizk. Temp. **31**, 752 (2005) [Low Temp. Phys. **31**, 569 (2005)].
[31]S. N. Shevchenko and A. N. Omelyanchouk, Fiz. Nizk. Temp. **32**, 1282 (2006) [Low Temp. Phys. **32**, 973 (2006)].
[32]V. I. Shnyrkov, Th. Wagner, D. Born, S. N. Shevchenko, W. Krech, A. N. Omelyanchouk, E. Il'ichev, and H.-G. Meyer, Phys. Rev. B **73**, 024506 (2006).
[33]W. D. Oliver, Y. Yu, J. C. Lee, K. K. Berggren, L. S. Levitov, and T. P. Orlando, Science **310**, 1653 (2005).
[34]G. Sun, X. Wen, Y. Wang, S. Cong, J. Chen, L. Kang, W. Xu, Y. Yu, S. Han, and P. Wu, Appl. Phys. Lett. **94**, 102502 (2005).
[35]M. Sillanpaa, T. Lehtinen, A. Paila, Yu. Makhlin, L. Roschier, and P. Hakonen, Phys. Rev. Lett. **95**, 206806 (2006).
[36]L. Du, D. Lan, and Y. Yu, Fiz. Nizk. Temp. **39**, 863 (2013) [Low Temp. Phys. **39**, 665 (2013)].
[37]Ya. S. Greenberg and E. Il'ichev, Phys. Rev. B **77**, 094513 (2008).
[38]V. I. Shnyrkov, D. Born, A. A. Soroka, and W. Krech, Phys. Rev. B **79**, 184522 (2009).
[39]S. N. Shevchenko, Eur. Phys. J. B **61**, 187 (2008).
[40]M. T. Tuominen, J. M. Hergenrother, T. S. Tighe, and M. Tinkham, Phys. Rev. Lett. **69**, 1997 (1992).
[41]Yu. Makhlin, G. Schön, and A. Shnirman, Rev. Mod. Phys. **73**, 357 (2001).
[42]M. Grajcar, S. H. W. van der Ploeg, A. Izmalkov, E. Il'ichev, H.-G. Meyer, A. Fedorov, A. Shnirman, and G. Schön, Nat. Phys. **4**, 612 (2008).
[43]V. P. Krainov and V. P. Yakovlev, Zh. Eksp. Teor. Fiz. **78**, 2204 (1980) [Sov. Phys. JETP **51**, 1104 (1980)].
[44]J. Q. You, Y. X. Liu, C. P. Sun, and F. Nori, Phys. Rev. B **75**, 104516 (2007).
[45]J. Hauss, A. Fedorov, C. Hutter, A. Shnirman, and G. Schön, Phys. Rev. Lett. **100**, 037003 (2008).
[46]J. C. Skinner, H. Prance, P. B. Stiffell, and R. J. Prance, Phys. Rev. Lett. **105**, 257002 (2010).
[47]A. M. Korolev, V. I. Shnyrkov, and V. M. Shulga, Rev. Sci. Instrum. **82**, 016101 (2011).
[48]O. Astafiev, Yu. A. Pashkin, Y. Nakamura, T. Yamamoto, and J. S. Tsai, Phys. Rev. Lett. **96**, 137001 (2006).
[49]F. Forster, G. Petersen, S. Manus, P. Hänggi, D. Schuh, W. Wegscheider, S. Kohler, and S. Ludwig, Phys. Rev. Lett. **112**, 116803 (2014).
[50]A. N. Omelyanchouk, E. V. Il'ichev, and S. N. Shevchenko, *Quantum Coherent Phenomena in Josephson Qubits* (Naukova Dumka, Kiev, 2013) (in Russian).

Translated by L. Gardt